Vol. **107** (2005) *ACTA PHYSICA POLONICA A* No. 1

Proceedings of the 12th International Symposium UFPS, Vilnius, Lithuania 2004

Ultrafast Phenomena in Freestanding LT-GaAs Devices

M. Marso[a,*], M. Mikulics[a,b], R. Adam[a], S. Wu[c], X. Zheng[c], I. Camara[b], F. Siebe[b], A. Förster[a], R. Güsten[b], P. Kordoš[a] and R. Sobolewski[c]

[a]Institute of Thin Films and Interfaces, Research Center Jülich
52425 Jülich, Germany

[b]Max-Planck-Institut für Radioastronomie, 53121 Bonn, Germany

[c]Department of Electrical and Computer Engineering and Laboratory for Laser Energetics
University of Rochester, Rochester, NY 14627-0231, USA

We report on the fabrication and high-frequency performance of our photodetectors and photomixers based on freestanding low-temperature--grown GaAs. The MBE-grown low-temperature GaAs layers are lifted from the native GaAs substrate and transferred on top of variety of host substrates. The freestanding devices exhibit breakdown electrical fields above 200 kV/cm and dark currents below 3×10^{-7} A at 100 V bias. Device photoresponse shows 0.55 ps wide electrical transients with voltage amplitudes up to 1.3 V, measured using an electro-optical sampling technique with 100 fs wide laser pulses. Photomixing experiments at 460 GHz yield a 9 times higher output power for the freestanding device on Si/SiO_2 host substrate compared to the native substrate.

PACS numbers: 72.20.Jv, 72.40.+w, 78.30.Fs, 85.60.–q, 85.60.Gz

1. Introduction

Low-temperature-grown GaAs (LT-GaAs) thin films exhibit subpicosecond carrier lifetime ($\sim$ 200 fs) [1], high resistivity ($> 10^7$ Ω cm) [2], high breakdown electric field ($>$ 300 kV/cm) [2], and relatively large mobility ($\sim$ 150 cm^2/(V s)) [3]. These properties make LT-GaAs the material of choice for fast and sensitive photodetectors [4–14] and photomixers [15–20]. Typically, LT-GaAs films are grown by molecular beam epitaxy in the temperature range from 200°C to 300°C, followed by rapid thermal annealing at 600°C [3, 6]. Artificially created deep-level

*corresponding author; e-mail: m.marso@fz-juelich.de

traps are responsible for the very short carrier lifetime in LT-GaAs based opto--electronic devices. LT-GaAs based photoconductors (PC) and photomixers emerge as devices in high demand for optical communication and for generation of high-power terahertz radiation. Electrical pulses in pico- and femtosecond region are being generated by pulsed laser illumination of a metal–semiconductor–metal (MSM) structure fabricated on top of the LT-GaAs surface [1]. Using optical-heterodyne conversion in LT-GaAs photomixing, several groups obtained impressive results with output power up to 3 μW at 460 GHz or 100 nW at 2 THz generated radiation [15–19]. Possible further improvement of photomixing output power is related to improved thermal dissipation by integration on substrates with high thermal conductivity [20]. Generally speaking the low thermal conductivity, the same bandgap as LT-GaAs, and the high costs of the GaAs substrate make a substrate desirable with properties that are more compatible with the designated applications. Integration of LT-GaAs into hybrid circuitry using flip-chip techniques or wire bonding has been used before, but such methods reduce the intrinsic multi-gigahertz bandwidth of the devices. A possible solution is an integration of (LT-) GaAs with a substrate using thin film epitaxial lift-off employing surface bonding through van der Waals forces. For successful LT-GaAs integration into practical electronic or optoelectronic circuits however, there is not only the need for a robust technique for a reliable LT-GaAs lift-off, transfer, and bonding, but also the size of the transferred structure must be microscopic, comparable with the size of the circuits components.

The aim of this work is to investigate fabrication and properties of hybrid devices consisting of SiO_2/Si or plastic substrates, integrated with micrometer-sized LT-GaAs that was epitaxially lifted and bonded at a predetermined substrate position. The use of Si as host substrate has strong practical implications, since Si is the most widely used semiconductor in electronics. In addition, Si has a higher thermal conductivity ($\alpha_{\mathrm{Si}} \approx 1.60$ W/cm/K) at room temperature than GaAs ($\alpha_{\mathrm{GaAs}} \approx 0.59$ W/cm/K), so using Si as the substrate should improve the high-power performance of optoelectronic devices, by enabling them to operate at higher excitation optical powers. Polyethylene terephthalate (PET) is an extremely interesting substrate due to its flexibility, high surface resistivity reaching $\sim 10^{13}$ Ω/sq, optical transparency and chemical stability [21–24]. Its integration with ultrafast photoswitches and photodetectors is expected to lead to the range of applications requiring high performance, low cost on-chip generators of terahertz radiation.

2. Fabrication

Both our photodetectors and photomixers are based on the freestanding LT-GaAs film. The LT-GaAs layers were fabricated using a commercial Varian Mod GEN II MBE system. We started with a 300 nm thick layer of AlAs on top of the GaAs substrate, followed by a 500 nm to 1.5 μm thick LT-GaAs film grown in

the temperature range of 200 to 300°C with a growth rate of about 1 μm/h [3, 6]. After the MBE deposition, wafers with LT-GaAs layers were annealed *in situ* at 600°C for 10 min under local As overpressure. The AlAs/LT-GaAs bilayer was subsequently patterned by photolithography and ion-beam etching to form a set of LT-GaAs microswitches, featuring sizes from 10×10 μm^2 to 150×150 μm^2 [20−26]. The LT-GaAs devices were next lifted from the GaAs substrate by selective chemical etching of the AlAs layer in diluted HF solution. After cleaning in de-ionized water, a selected microswitch was transferred on top of a chosen substrate using a metallic tip, electrostatically charged and electrically isolated from the ground [20]. The release process was achieved by using a second metallic tip, which was connected to ground, thus, providing a route for the charge release after the devices were placed at their designated positions, where they were fixed by van der Waals attraction [27, 28]. To minimize the height difference between the switch and the substrate surfaces, the host substrates contained 500 nm deep, ion-etched "wells" matching the microswitch, pre-positioned at the designated position. Following the microswitch transfer, continuous coplanar lines crossing the devices were fabricated using Ti/Au deposition and a standard lift-off technique. A micrograph of one of our devices is shown in Fig. 1. For photomixer fabrication a set of MSM

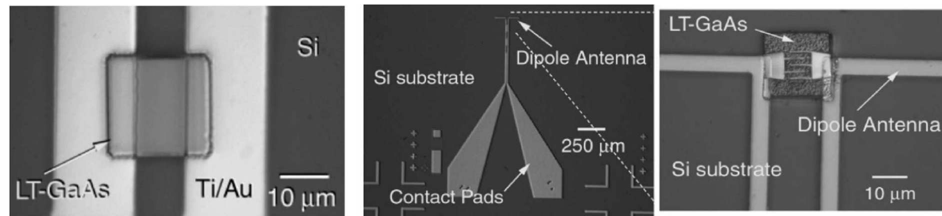

Fig. 1. Photograph of an Au/Ti CPS transmission line with a 20×20 μm^2 LT-GaAs microswitch placed in the CPS gap (left). Microscope picture of the photomixer fabricated on the silicon substrate integrated with the freestanding 20×20 μm^2 LT-GaAs layer, 8×8 μm^2 LT-GaAs/MSM interdigitated structure integrated with 460 GHz dipole antenna (middle, right).

interdigitated finger structures was prepared on top of the LT-GaAs using conventional lift-off process, prior to the ion-beam etching and epitaxial lift-off from the native substrate. Finger width and spacing of the MSM structure were typically 200 nm and 1.8 μm, respectively. Following the transfer of LT- -GaAs on the top of a chosen substrate, conventional lift-off was used to connect LT-GaAs/MSM with 460 GHz tuned single dipole antenna and with coplanar lines containing low-pas filters and serving to provide dc bias leads. Figure 1 shows the micrograph of an LT-GaAs/MSM photomixer layout with interdigitated structure integrated with a 460 GHz dipole antenna, respectively.

3. Results and discussions

Figure 2 shows typical current–voltage ($I-V$) characteristics of freestanding LT-GaAs transferred on top of a sapphire, Si/SiO_2, and PET plastic substrates [20], as well as for as-grown LT-GaAs on native GaAs substrate, measured in the dark. The as-grown samples exhibit ohmic dependence up to $\sim$ 10 V and at higher bias nonlinear behavior is observed. On the other hand, the freestanding devices transferred on top of a host substrate show ohmic behavior in the whole range of applied voltages up to 200 V (corresponding to an average electric field of 200 kV/cm). Furthermore, Fig. 2 demonstrates that our freestanding structures exhibit more than 10-fold decrease of the dark current as compared to the as-grown devices, and they show no sign of electrical breakdown up to 200 V of dc bias. This improvement shows the advantage of the insulating host substrates compared to the semi-insulating GaAs native substrate.

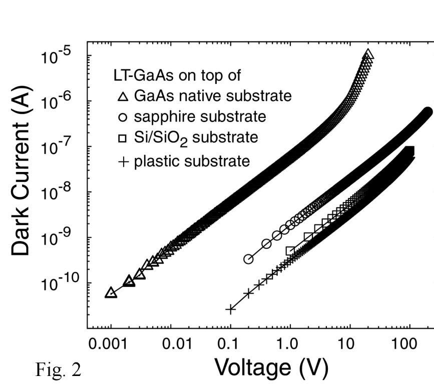

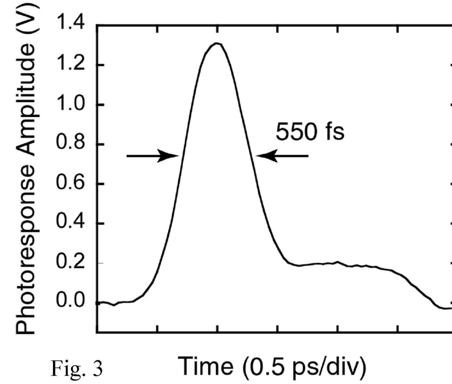

Fig. 2. $I-V$ characteristics of an as-grown LT-GaAs-on-GaAs device and the LT-GaAs microswitch transferred on top of the sapphire, Si/SiO_2, and PET plastic substrates.
Fig. 3. 550 fs FWHM photoresponse of a freestanding LT-GaAs switch exposed to 100 fs wide, 810 nm wavelength optical pulses, at 92 V bias and 2 mW input power.

The time-resolved photoresponse of the freestanding LT-GaAs microswitches was measured using electro-optic sampling [29–31] with 100 fs wide optical pulses from a Ti:sapphire laser at 810 nm wavelength. The transients were sampled with the spot located only $\sim$ 50 μm away from the device. Thus, the signal distortion caused by pulse dispersion effects in the coplanar lines was minimized enabling the measurement of near-to-intrinsic carrier dynamics in the LT-GaAs films. The time-resolved photoresponse signal of a freestanding LT-GaAs switch transferred on the Si/SiO_2 substrate and illuminated by 810 nm photons is shown in Fig. 3. The transient exhibits a 550 fs full-width-at-half-maximum (FWHM) photoresponse, that is nearly identical to a previously measured value of 580 fs for an LT-GaAs photodetector on its native GaAs substrate [1].

The photoresponse amplitude increases linearly with increasing photoexcitation power P_{ex}. Above 2 mW, however, the signal amplitude starts to level off. We believe that the saturation arises due to the fact that at a threshold P_{ex} all carriers for a given photon energy are excited which leads to the so-called band filling effect. When the free carrier density becomes too high, space-charge effect can contribute to the onset of saturation by affecting the carrier mobility in the conduction band. The decrease of the carrier collection efficiency can also be illustrated by measuring the dc responsivity that is defined as the ratio of the photocurrent and the input optical power. The voltage responsivity measured at a bias of 30 V decreases from 25 V/W at 1 mW to 10 V/W at 7 mW optical input power [20].

Figure 4 shows the response amplitude and response time as a function of applied bias, measured at the excitation power of ~ 0.46 mW. The pulse amplitude increases linearly at low voltages, and at higher biases the amplitude saturates, indicating a decrease of carrier collection efficiency. Closed circles illustrate constant photoresponse time of our devices for biases up to 120 V. For comparison, open circles indicate data from Ref. [32] performed on an LT-GaAs switch on native GaAs substrate. The considerable increase of the response time for high electric fields, in contrast to the freestanding device, can be explained by thermal effects due to the lower thermal conductivity of GaAs [14] or by the penetration of the electric field into the GaAs substrate where slow carriers can be excited [20].

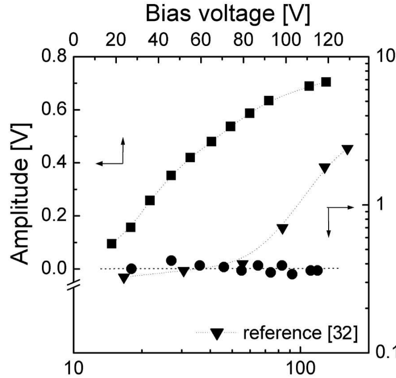

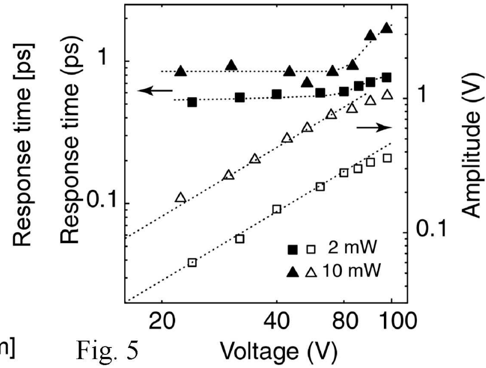

Fig. 4. Response time as a function of an average electric field (right and bottom axes) and amplitude as a function of applied bias voltage (left and upper axes) for LT-GaAs--on-Si microswitch. Curve marked by triangles shows response times for LT-GaAs--on-GaAs given in [32].

Fig. 5. Response time and amplitude of electrical transients of the LT-GaAs-on-PET photodetector as a function of bias voltage for 2 and 10 mW optical power. The dotted lines are guides for eye.

The LT-GaAs-on-PET devices were first characterized by $I-V$ measurements in the dark and under the 850 nm continuous-wave illumination. The $I-V$ curves exhibit ohmic behavior up to 70 V. The space-charge effect is not observed, which indicates efficient suppression of high-field region near the contacts. The devices exhibit low dark currents of 6×10^{-9} A at 10 V and $\leq 10^{-7}$ A at 100 V, and show breakdown voltages in the range from 110 V to 130 V. The results from electro-optic sampling measurements yield 0.7 ps FWHM response time, comparable to reported values on freestanding LT-GaAs on Si/SiO_2 [28]. Device response time and amplitude as a function of applied bias voltage are shown in Fig. 5. Response times down to 0.55 ps and amplitudes up to 1 V have been achieved [33]. In the low voltage bias region the response time is constant and the amplitude increases proportionally with the bias, as one would expect. On the other hand, the response time increases and the amplitude saturates if the bias voltage is increased above 70–75 V. This indicates the influence of heating effects at higher biases that become apparent due to the very low thermal conductivity of PET substrate (1.5 mW cm^{-1} K^{-1}). Measurements at increased illumination power confirm the above result that heating effects do not play a significant role at biases below 70–75 V. However, for 97 V bias voltage and 10 mW input power an increase of the response time reached 1.7 ps thus supporting the effect explanation by overheating.

Photomixer experiments were performed by an experimental setup with two tunable semiconductor lasers operated at 780 nm wavelength that are coupled to an optical amplifier. A part of the amplifier output signal is monitored by a wavemeter to determine the difference frequency between the two lasers. The rest is coupled to a monomode fiber optic and directed to the photodetector area of the photomixer. The applied bias generates a photocurrent that is modulated with the frequency difference of the two lasers. A Golay cell allows the measurement of the power of the generated radiation that is emitted by the dipole antenna. The above-mentioned improvements in thermal management of our freestanding photoconducting devices should lead to an increase of the photomixer output power. One example of the working device is shown in Fig. 1 showing the photomixer device with 20×20 μm^2 LT-GaAs layer with thickness about 1 μm on the silicon substrate coupled with dipole antenna. We used silicon substrate because of its 3-times higher thermal conductivity in comparison with the native GaAs substrate. As shown in Fig. 6, at low photomixer bias, we observed output power exceeding 9-times the output power of the devices fabricated on native GaAs substrate [34]. We ascribe the improvement to the better thermal management of the device. At higher voltages, corresponding to the approximately 12 kV/cm average electric field, however, electrical breakdown occurred due to not fully optimized electrical contact in the LT-GaAs-metallization interface. We believe that improvements in device fabrication technique will lead to future increase of the device output exceeding the current in best devices on native GaAs.

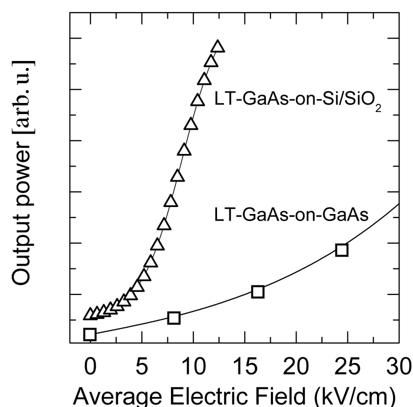

Fig. 6. Comparison of output power at 460 GHz from photomixers based on LT-GaAs on native GaAs and LT-GaAs on silicon substrates.

4. Conclusions

We selectively etched 20×20 μm^2 LT-GaAs thin-film square pieces and transferred them on top of Si/SiO_2, sapphire, and plastic (polyethylene terephthalate) substrates. The thin films were subsequently integrated with metallic transmission lines, forming freestanding photoconductive microswitches and high-frequency photomixers. The freestanding devices exhibited 10-fold lower dark currents and higher breakdown voltages as compared to devices patterned on native GaAs substrates. High saturation voltage and the linear dependence of the photoresponse amplitude on the bias voltage for both photoconductive switches and photomixing devices result from high quality contacts formed between our freestanding LT-GaAs films and the metallic electrodes. Electro-optic sampling measurements showed 0.55 ps wide response at 810 nm wavelength excitation, with up to 1.3 V photoresponse amplitude and above 10^3 V/W responsivity. The output power of the freestanding LT-GaAs-on-Si photomixers was measured using two-laser heterodyne mixing at 460 GHz and showed ninefold increase of the output power in low voltage bias region compared to the devices fabricated on top of GaAs substrates.

Our technique is also applicable for other host substrates, as substrates with large bandgap as well as with high thermal conductivity. While the latter results in more efficient device cooling, large bandgap enables device biasing at higher electric field intensities without carrier collection from the substrate. Sapphire and MgO are extremely attractive substrate materials suitable for cryogenic applications due to their compatibility with high-temperature superconductors. Integration of LT-GaAs with transparent substrates, such as MgO, sapphire, and PET, allows experiments in the transmission mode, e.g., optical excitation of devices through the substrate. In summary, the freestanding LT-GaAs microswitches are suitable

for hybrid optoelectronic applications, on-chip femtosecond-pulse generators, as well as for low-cost high-power terahertz frequency generators that can be placed at any chosen position of the electronic circuit.

References

[1] P. Kordoš, A. Föster, M. Marso, F. Rüders, *Electron. Lett.* **34**, 119 (1998).

[2] D.C. Look, *Thin Solid Films* **231**, 61 (1993).

[3] P. Kordoš, M. Marso, A. Föster, J. Darmo, J. Betko, G. Nimtz, *Appl. Phys. Lett.* **71**, 1118 (1997).

[4] S. Gupta, J. Whitaker, G. Mourou, *IEEE J. Quantum Electron.* **28**, 2464 (1992).

[5] J.F. Whitaker, *Mater. Sci. Eng. B* **22**, 61 (1993).

[6] J. Betko, M. Morvic, J. Novak, A. Förster, P. Kordoš, *J. Appl. Phys.* **86**, 6243 (1999).

[7] S. Gupta, M.Y. Frankel, J.A. Valdmanis, J.F. Whitaker, G.A. Mourou, F.W. Smith, A.R. Calawa, *Appl. Phys. Lett.* **59**, 3276 (1991).

[8] Y.-J. Chiu, S.B. Fleischer, D. Lasaosa, J.E. Bowers, *Appl. Phys. Lett.* **71**, 2508 (1997).

[9] M.Y. Liu, S.Y. Chou, T.Y. Hsiang, S. Alexandrou, R. Sobolewski, *J. Vac. Sci. Technol. B* **10**, 2832 (1992).

[10] K. Kato, *IEEE Trans. Microw. Theory Tech.* **47**, 1265 (1999).

[11] S.Y. Chou, Y. Liu, P.B. Fischer, *Appl. Phys. Lett.* **61**, 819 (1992).

[12] D. Krökel, D. Grischkowsky, M.B. Ketchen, *Appl. Phys. Lett.* **54**, 1046 (1989).

[13] E. Sano, T. Shibata, *Appl. Phys. Lett.* **55**, 2748 (1989).

[14] M.Y. Frankel, J.F. Whitaker, G.A. Mourou, F.W. Smith, A.R. Calawa, *IEEE Trans. Electron Devices* **37**, 2493 (1990).

[15] E.R. Brown, K.A. McIntosh, K.B. Nichols, C.L. Dennis, *Appl. Phys. Lett.* **66**, 285 (1995).

[16] A.S. Pine, R.D. Suenram, E.R. Brown, K.A. McIntosh, *J. Mol. Spectrosc.* **175**, 37 (1996).

[17] E. Peytavit, G. Mouret, J.F. Lampin, P. Masselin, P. Mounaix, F. Mollot, D. Lippens, in: *Proc. 8th Intern. Conf. on Terahertz Electronics September 2000, Darmstadt (Germany).*

[18] E. Peytavit, S. Arscott, D. Lippens, G. Mouret, S. Matton, P. Masselin, R. Bocquet, J.F. Lampin, L. Desplanque, F. Mollot *Appl. Phys. Lett.* **81**, 1174 (2002).

[19] S. Matsuura, M. Tani, K. Sakai, *Appl. Phys. Lett.* **70**, 59 (1997).

[20] M. Mikulics, Ph.D. Thesis, Research Center Jülich, Jülich 2004.

[21] R. Paetzold, K. Heuser, D. Henseler, S. Roeger, *Appl. Phys. Lett.* **82**, 3342 (2003).

[22] P. Kus, A. Plecenik, L. Satrapinsky, Y. Xu, R. Sobolewski, *Appl. Phys. Lett.* **81**, 2199 (2002).

[23] Y. Ichikawa, T. Yoshida, T. Hama, H. Sakai, K. Harashima, *Solar Energy Mat. & Solar Cells* **66**, 107 (2001).

[24] H. Jia, J. Veldeman, M. Burgelman, *J. Magn. Magn. Mater.* **223**, 73 (2001).

[25] E. Yablonovitch, T. Gmitter, J.P. Harbison, R. Bhat, *Appl. Phys. Lett.* **51**, 2222 (1987).

[26] E. Yablonovitch, D.M. Hwang, T.J. Gmitter, L.T. Florez, J.P. Harbison, *Appl. Phys. Lett.* **56**, 2419 (1990).

[27] M. Mikulics, M. Marso, R. Adam, A. Fox, D. Buca, A. Förster, P. Kordoš, in: *2001 Intern. Symp. on Electron Devices for Microwave and Optoelectronic Applications, Vienna, November 2001, Proc. 9th EDMO, IEEE Catalog Number*: 01TH8567, ISBN: 0-7803-7049-X, 155 (2001).

[28] R. Adam, M. Mikulics, A. Förster, J. Schelten, P. Kordoš, M. Siegel, X. Zheng, S. Wu, R. Sobolewski, *Appl. Phys. Lett.* **81**, 3485 (2002).

[29] J.A. Valdmanis, G.A. Mourou, *IEEE J. Quantum Electron.* **QE-22**, 69 (1986).

[30] M.Y. Frankel, J.F. Whitaker, G.A. Mourou, J.A. Valdmanis, *IEEE Microw. Guided Wave Lett.* **1**, 60 (1991).

[31] R. Adam, R. Sobolewski, M. Darula, *Proc. SPIE* **4058**, 230 (2000).

[32] N. Zamdmer, Q. Hu, K.A. McIntosh, S. Verghese, *Appl. Phys. Lett.* **75**, 2313 (1999).

[33] M. Mikulics, R. Adam, M. Marso, A. Förster, P. Kordoš, S. Wu, X. Zheng, R. Sobolewski, submitted to *Appl. Phys. Lett.*

[34] M. Mikulics, F. Siebe, X. Zheng, R. Adam, M. Marso, H. Stüer, R. Sobolewski, R. Güsten, P. Kordoš, in: *4th Symp. on Non-Stoichiometric III–V Compounds, October 2002, Asilomar (USA).*